

A gas-phase solvent effect: The role of water molecules in the conversion of the $\text{HOMg}^+/\text{CO}_2$ adduct ion to the magnesium bicarbonate ion, $\text{Mg}^+\text{O}_2\text{COH}$

Simon Petrie*

Department of Chemistry, College of Science, the Australian National University, Canberra ACT 0200, Australia

Received 30 January 2006; received in revised form 5 June 2006; accepted 5 June 2006

Available online 10 July 2006

Abstract

Quantum chemical calculations at the CP-dG2thaw and MP2(thaw)/B4G levels of theory are reported for the bare HOMg^+OCO ion resulting from addition of CO_2 to HOMg^+ , and to its mono-, di- and tri-hydrated forms. These calculations are used to determine bond dissociation energy (BDE) values for the $(\text{H}_2\text{O})_n(\text{CO}_2)_i\text{HOMg}^+-\text{OH}_2$ ($n=0-2$; $i=0, 1$) and $(\text{H}_2\text{O})_n\text{HOMg}^+-\text{OCO}$ ($n=0-3$) bonds, as well as to ascertain the relative energies for several key stationary points on each of the $\text{HOMg}^+(\text{H}_2\text{O})_n\text{CO}_2$ ($n=0-3$) potential energy surfaces. Three principal findings emerge from these calculations. First, in contrast to the isoelectronic system $\text{NaOH} + \text{CO}_2 \rightarrow \text{NaO}_2\text{COH}$ held to play a leading role in noctilucent cloud nucleation, the reaction of $\text{HOMg}^+ + \text{CO}_2$ does not result in formation of the magnesium bicarbonate cation $\text{Mg}^+\text{O}_2\text{COH}$. Second, the cumulative Mg^+ -ligand bond energies for complexes of HOMg^+ with several H_2O and CO_2 molecules rapidly approach, and then exceed, the available Mg^+ recombination energy, indicating that dissociative recombination of $\text{HOMg}^+(\text{H}_2\text{O})_n\text{CO}_2$ (or its bicarbonate-containing isomer $\text{Mg}^+\text{O}_2\text{COH}(\text{H}_2\text{O})_n$) is likely to result in the production of molecular Mg-containing neutrals. Third, we find that hydration exhibits a remarkable influence on the reactivity of HOMg^+ with mesospheric CO_2 : addition of CO_2 to bare HOMg^+ does not result in bicarbonate formation, nor do the reactions of HOMg^+CO_2 and $\text{HOMg}^+\text{OH}_2\text{CO}_2$ with H_2O , but the reaction of $\text{HOMg}^+(\text{OH}_2)_2\text{CO}_2$ with H_2O leads to two possible bicarbonate-containing products $(\text{H}_2\text{O})_2\text{Mg}^+\text{O}_2\text{COH}$ and $(\text{H}_2\text{O})_3\text{Mg}^+\text{O}_2\text{COH}$. The former product channel, which involves association followed by H_2O loss, is judged to be an unusual example of a catalytic process in which the principal contribution of the H_2O 'catalyst' is steric.

© 2006 Elsevier B.V. All rights reserved.

Keywords: Atmospheric chemistry; Bicarbonate formation; Ion catalysis; Ion–ligand binding; Main-group metal ion; Meteoric ablation; Quantum chemical calculation; Solvent-assisted reaction

1. Introduction

One of the key routes to noctilucent cloud nucleation [1], at a typical altitude of ~ 85 km, is held to be the reaction [1,2] between gas-phase NaOH and CO_2 :



The sodium bicarbonate product of this reaction is highly resistant to chemical and photochemical degradation [1], and is lost principally through a progressive hydration process [1,3] (ultimately leading to particles large enough to be effectively self-sustaining, and constituting the cloud nucleation sites in

question). Several pathways to the sodium hydroxide reactant, from the reactions of the meteoric ablation products Na and Na^+ with various atmospheric species, are known to exist [4–7].

We have recently proposed [8] that HOMg^+ , a species isoelectronic with NaOH , is an important intermediate in the mesospheric processing of ablated meteoric magnesium ions. As with NaOH , HOMg^+ appears to be very robust and resistant to chemical degradation (i.e., ligand switching and ligand stripping) by known mesospheric constituents [8], and there are several feasible pathways by which HOMg^+ can arise within the mesosphere. One such process, the reaction of MgO^+ with H_2O , has in fact been known to the ion chemistry community for many years, and has been determined to occur with near-collisional efficiency according to flow tube measurements at 300 K [9]; however, this reaction appears not to have been considered within models of mesospheric metal ion chemistry [10–13] until very recently

* Tel.: +61 2 6125 7931; fax: +61 2 6125 0760.
E-mail address: simon.petrie@anu.edu.au.

[8]. Intrigued by the structural similarity between NaOH and HOMg^+ , we have set out to determine how far the chemical analogy extends, in the context of possible bicarbonate formation also in the reaction of HOMg^+ with CO_2 :



As in several previous studies of metal ion chemistry and thermochemistry [8,14–21], the species investigated in the present work have been characterized, where feasible, by a high-level composite quantum chemical method, CP-dG2thaw [22,23], which has been specifically tailored to deliver high-accuracy results for main-group-metal-containing molecules and molecular ions.

2. Theoretical methods

The CP-dG2thaw method [22,23] has been employed wherever practicable in the calculations reported herein. This quantum chemical method is an adaptation of the widely-used Gaussian-2 (G2) approach [24]. The modifications to the standard G2 method which are inherent in CP-dG2thaw are the omission of G2's empirical 'higher level correction' (HLC) [24], the substitution of a partially-decontracted metal atom basis set [22] for the standard 6-311 + G (3df,2p) basis employed by G2 [24], the implementation [22,25] of a counterpoise correction [26] for basis set superposition error (BSSE), and the inclusion of metal-based 'inner-valence' electrons (here Mg 2s and 2p) within the correlation space in all correlated calculation steps [27]. The CP-dG2thaw method also adopts optimized geometries, vibrational frequencies, and (uncorrected) zero-point vibrational energy (ZPE) determinations obtained using the widely-used hybrid density functional method B3-LYP [28,29] which here is combined with the polarization- and diffuse-function-augmented triple-split-valence Gaussian-function basis set 6-311 + G**. The rationale behind these various modifications to standard G2 [24] has been repeatedly presented in several previous works [22,23,27] and is not reiterated here. A justification for these modifications can, however, be succinctly expressed: in the context of sodium ion complexation free energies to various ligands, which arguably constitute the most extensive and precise data set of gas-phase metal ion/ligand thermochemical values yet measured [30,31], CP-dG2thaw delivers near-perfect agreement [21,22] with the relative free energy ladder [30] and only marginally poorer agreement with the established absolute 'anchor' value of $\Delta G_{298}^\circ(\text{Na}^+ - \text{NH}_2\text{CH}_3)$ [32]. To the best of our knowledge, no other quantum chemical method has yet shown such consistently good accord with the primary experimental data set for main-group metal ion/ligand thermochemistry [31].

For several of the structures reported here, calculations at the CP-dG2thaw level were not feasible due to limitations of the available computational platforms. In such cases, which comprise all of the doubly- and triply-hydrated complexes containing also CO_2 , calculation at the CP-MP2(thaw)/B4G level of theory were pursued. This more modest level of theory shares with CP-dG2thaw [22,23] the treatment of BSSE, the inclusion of inner-valence correlation, and the use of B3-LYP/6-311 + G** optimized geometries and zero-point vibrational energies; it also

uses the largest basis set employed in the CP-dG2thaw method, but omits the treatment of electron correlation to higher order than MP2. The CP-MP2(thaw)/B4G method has been shown to deliver generally close agreement with CP-dG2thaw on calculated bond dissociation energies (BDEs) of Mg^+ -containing ions [8,33].

In both the CP-dG2thaw and CP-MP2(thaw)/B4G methods, counterpoise corrections for BSSE are obtained at the MP2(thaw)/B4G level of theory. The counterpoise correction for BSSE for an N -body cluster is not uniquely defined [34–36], nor is there consensus on which of several algorithms provides the most meaningful correction. Here we have adopted the site-site function counterpoise (SSFC) method of Wells and Wilson [34], which is computationally the most easily implemented method for obtaining N -body counterpoise corrections. This method has been adopted in all of the determinations of BDEs for water ligands reported here, and for BDEs involving straightforwardly bound CO_2 . For the BDE values for liberation of CO_2 from bicarbonate-containing structures, no direct counterpoise correction has been applied. Instead, the appropriate counterpoise correction is assumed to equate to that determined for CO_2 loss from the isomeric $\text{HOMg}^+ \cdot (\text{OH}_2)_n \cdot \text{CO}_2$ cluster ion. While this assumption may not be completely valid, it appears less questionable than the alternative counterpoise approach of treating the HO and CO_2 moieties within the bicarbonate ligand as separate, weakly interacting entities.

All calculations reported here were performed using the GAUSSIAN98 [37] and GAUSSIAN03 [38] program suites.

3. Results and discussion

3.1. Adduct ion structures and energetics for the species $\text{Mg}^+ \cdot (\text{H}_2\text{O})_n \text{CO}_2$ and $\text{HOMg}^+ \cdot (\text{H}_2\text{O})_n \cdot (\text{CO}_2)_i$ ($n = 0-2$, $i = 0, 1$)

Total energies and BDE values for bare and hydrated Mg^+ , Mg^+OCO , HOMg^+ , and HOMg^+OCO are detailed in Table 1. Structures for the bare to doubly-hydrated CO_2 -containing species are shown in Fig. 1. Several energetic and structural trends are readily apparent from perusal of the table and figure. For example, increasing hydration consistently results in a modest progressive lengthening and significant weakening of each Mg^+ /ligand interaction: this is consistent with the influence of ligand/ligand repulsion within the complexes, as well as the tendency for charge delocalization through the partially-covalent interaction between Mg^+ and H_2O . Conversely, derivatization of the magnesium ion by the hydroxyl ligand has a quite dramatic impact on the BDEs of other ligands, increasing each $\text{BDE}(\text{Mg}^+ - \text{OH}_2)$ value by around 50%, and raising the $\text{BDE}(\text{Mg}^+ - \text{OCO})$ values by 100% or more in several instances. This dramatic enhancement in bond strengths results from the highly polar Mg^+/OH interaction, which formally increases the oxidation number of Mg from a nominal value of 1 to a value typically between 1.7 and 1.8 (as assessed by the atomic Mulliken charges) and therefore strengthens the ion/dipole and ion/induced dipole interactions between magnesium and the other ligands. This phenomenon, and its implications for atmo-

Table 1
Total energies and bond dissociation energies of Mg-containing ions

Ion	E_0 (Hartree) ^a		BDE (kJ mol ⁻¹) ^d	
	MP2 ^b	dG2thaw ^c	XMg ⁺ -OH ₂ ^e	XMg ⁺ -OCO ^c
Mg ⁺	-199.50178	-199.50347	–	–
Mg ⁺ ·OH ₂	-275.84700	-275.86337	121.8/ 122.4 ^f	–
Mg ⁺ ·(OH ₂) ₂	-352.18313	-352.21428	97.4/ 98.4	–
Mg ⁺ ·(OH ₂) ₃	-428.51364	-428.55967	81.2/ 82.4	–
Mg ⁺ ·CO ₂	-387.82571	-387.84991	–	58.3/ 60.8 ^f
Mg ⁺ ·OH ₂ ·CO ₂	-464.16456	-464.20332	104.9/ 105.2	41.4/ 43.6
Mg ⁺ ·(OH ₂) ₂ ·CO ₂	-540.49646	–	85.4	29.3
Mg ⁺ ·(OH ₂) ₃ ·CO ₂ (“4,0”)	-616.82292	–	72.6	20.7
Mg ⁺ ·(OH ₂) ₃ ·CO ₂ (“3,1”)	-616.82232	–	71.3	19.5
HOMg ⁺	-275.24004	-275.25254	–	–
HOMg ⁺ ·OH ₂	-351.61561	-351.64225	199.5/ 198.7 ^f	–
HOMg ⁺ ·(OH ₂) ₂	-427.97265	-428.01400	151.5/ 152.3	–
HOMg ⁺ ·(OH ₂) ₃	-504.31776	-504.37389	116.9/ 117.9	–
HOMg ⁺ ·CO ₂	-463.59220	-463.62702	–	130.3/ 132.4 ^f
HOMg ⁺ ·OH ₂ ·CO ₂	-539.95117	-540.00051	156.7/ 156.9	87.6/ 90.6
HOMg ⁺ ·(OH ₂) ₂ ·CO ₂	-616.29865	–	123.8	59.8
HOMg ⁺ ·(OH ₂) ₃ ·CO ₂ (“5,0”)	-692.63330	–	89.4	32.2
HOMg ⁺ ·(OH ₂) ₃ ·CO ₂ (“4,1”)	-692.62774	–	77.6	20.5
Bicarbonate formation TS	-692.62602	–	66.1	8.9
Mg ⁺ O ₂ COH	-463.57547	-463.61491	–	86.4/100.6
H ₂ O·Mg ⁺ O ₂ COH	-539.94801	-540.00164	191.1/ 190.4 ^g	79.3/93.5
(H ₂ O) ₂ ·Mg ⁺ O ₂ COH	-616.30320	–	145.1 ^g	71.8
(H ₂ O) ₃ ·Mg ⁺ O ₂ COH #1	-692.62807	–	63.4 ^g	18.5
(H ₂ O) ₃ ·Mg ⁺ O ₂ COH #2	-692.64664	–	112.1 ^g	67.3
(H ₂ O) ₃ ·Mg ⁺ O ₂ COH TS “A” (#1 ↔ #2)	-692.61943	–	41.0 ^g	-4.2
(H ₂ O) ₃ ·Mg ⁺ O ₂ COH TS “B” (#1 ↔ #2)	-692.58564	–	-48.3 ^g	-92.9

^a Total energy, at 0 K, determined at the indicated level of theory, including zero-point energy calculated at the B3-LYP/6-311 + G** level of theory.

^b MP2(thaw)/B4G level of theory. See text for details.

^c dG2thaw level of theory. See text for details.

^d Bond dissociation energy at 0 K, including zero-point energy (at the B3-LYP/6-311 + G** level) and a counterpoise correction for BSSE (at the MP2(thaw)/B4G level). The first BDE value shown is calculated at the CP-MP2(thaw)/B4G level of theory; the second value, where shown, is at the CP-dG2thaw level. The latter value is shown in bold, *except* when the BDE calculation is indirect (see text for details).

^e BDE for removal of H₂O or CO₂ from the identified complex ion.

^f Previously reported in Ref. [8].

^g BDE calculated assuming the bicarbonate ligand remains intact in the dehydrated cluster ion.

spheric Mg⁺ chemistry, have been noted previously [8], while laboratory validation of a very similar trend has been reported for the BDEs of Mg⁺ versus CIMg⁺ [39].

It is worth comparing the interaction of HOMg⁺ and CO₂ with the analogous NaOH/CO₂ reaction [1,2]. Calculations on the various [NaHCO₃] stationary points, at the CP-MP2(thaw)/B4G level of theory [19], indicate that sodium bicarbonate is produced through the barrierless formation of a chelated intermediate **1** which can then rearrange to the more stable isomer **2** (see Fig. 2) by two competing mechanisms: H-atom migration, and metal-atom migration. The transition states for these mechanisms are shown in Fig. 2 as, respectively, TS ‘A’ and ‘B’. Of the two mechanisms, the barrier to Na atom migration is by far the lower, and lies substantially below the total energy of reactant NaOH + CO₂ at the CP-MP2(thaw)/B4G level of theory, whereas the barrier represented by TS ‘A’ protrudes significantly above the total energy of reactants. The structures **1**, TS ‘A’, and TS ‘B’ have no locatable counterparts on the HOMg⁺/CO₂ reaction potential energy surface, nor on the analogous singly- and doubly-hydrated surfaces. The absence of the

key reaction intermediate **1** in the HOMg⁺/CO₂ reaction implies that bicarbonate formation cannot proceed through straightforward bond formation between ligated hydroxide and the CO₂ carbon as is the case in the NaOH/CO₂ reaction. Furthermore, our efforts to locate any other transition state structures leading to Mg⁺O₂COH formation – for example, by hydroxide detachment and migration – have also been unsuccessful. It would appear that, while the closed-shell neutral/neutral reaction of NaOH + CO₂ gives a bicarbonate product through a process lacking an overall activation energy barrier, the analogous process in the ion/molecule reaction HOMg⁺ + CO₂ (although still exothermic as established by the thermochemical data in Table 1) is too highly inhibited to occur. This observation turns on its head the conventional wisdom, often stated in the literature, that *ion/molecule reactions very often lack the barriers encountered in the analogous reactions between closed-shell neutrals, because of the strong long-range ion/dipole and ion/induced dipole attractive interactions in the ionized systems.*

Of course, NaOH is in some respects an atypical closed-shell reactant, and is best viewed as Na⁺OH⁻ in the same way that

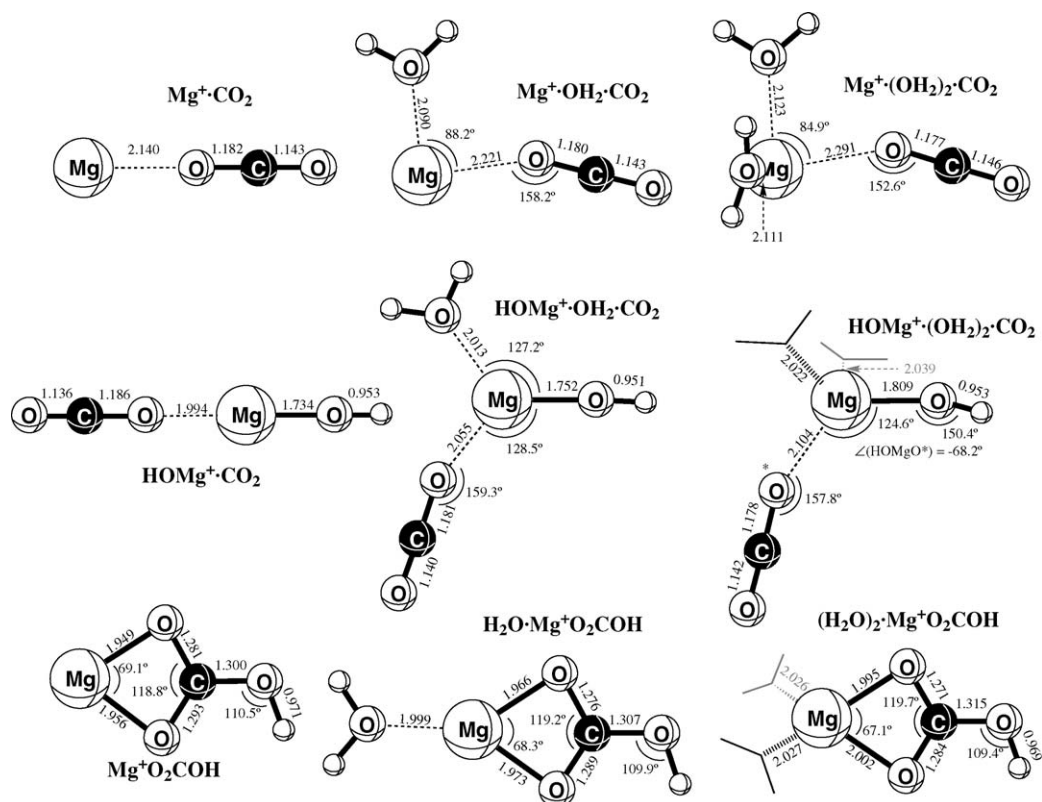


Fig. 1. Optimized geometries, obtained at the B3-LYP/6-311+G** level of theory, of relevant minima and transition states of the structures $\text{Mg}^+(\text{OH}_2)_n\text{CO}_2$, $\text{HOMg}^+(\text{OH}_2)_n\text{CO}_2$, and $(\text{H}_2\text{O})_n\text{Mg}^+\text{O}_2\text{COH}$, $n=0-2$. Bond lengths are shown in Ångströms and bond angles in degrees. For the $n=2$ structures, out-of-plane water ligands are shown simply in stick form for simplicity; when such ligands lie behind the plane of the page, they are shown in half-tone.

HOMg^+ has the chemical character of $\text{Mg}^{2+}\text{OH}^-$. The failure of bicarbonate formation in the $\text{HOMg}^+/\text{CO}_2$ interaction can therefore be interpreted as a consequence of the significantly stronger close-range interaction between a dicationic metal ion and its associated ligands OH^- and CO_2 , versus the analogous interaction between monocationic Na^+ and the OH^- and CO_2 ligands. A linear structure of the formula $\text{OCO}\cdot\text{NaOH}$ can in fact be isolated at the B3-LYP/6-311+G** level of theory, but it is found to be a second-order saddle point which rearranges spontaneously to structure **1** once symmetry constraints are relaxed. In contrast, the analogous linear structure in the $\text{HOMg}^+/\text{CO}_2$ system (see Fig. 1) is the global minimum on its potential energy surface, stabilized by over 30 kJ mol^{-1} relative to the bicarbonate isomer $\text{Mg}^+\text{O}_2\text{COH}$ according to our CP-dG2thaw calculations. It appears that the impediment to $\text{Mg}^+\text{O}_2\text{COH}$ formation is the relatively high strength of the interaction between HOMg^+ and CO_2 as a discrete ligand, which makes CO_2 incorporation into the

bicarbonate ligand energetically unfavorable as well as mechanically unattainable.

At this point, it is relevant to note that although there is generally good agreement between the CP-MP2(thaw)/B4G and CP-dG2thaw BDE values in Table 1, there is a significant discrepancy evident in the BDE values for CO_2 within $\text{Mg}^+\text{O}_2\text{COH}$ and $\text{H}_2\text{O}\cdot\text{Mg}^+\text{O}_2\text{COH}$. For both of these structures the CP-dG2thaw BDE (which we expect to be the more reliable value because of its more extensive treatment of electron correlation) is 14.2 kJ mol^{-1} larger than the corresponding CP-MP2(thaw)/B4G value. The consistency of the difference between the two levels of theory for these species, and the very good agreement evident between these methods for the other species surveyed here, suggests that the CP-MP2(thaw)/B4G method provides erroneous results for the energies of bicarbonate-containing structures investigated here. While it is not currently feasible to pursue CP-dG2thaw cal-

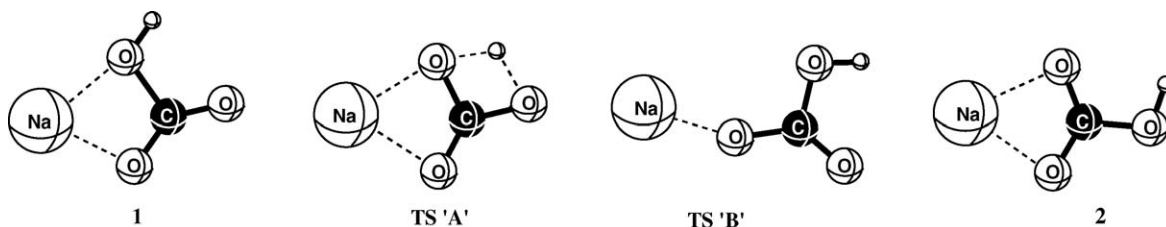


Fig. 2. Structures involved in formation of the NaHCO_3 global minimum **2**, in the reaction between NaOH and CO_2 .

culations on the more heavily hydrated bicarbonate-containing structures in Table 1, we consider it likely that the $\sim 14 \text{ kJ mol}^{-1}$ difference between the two methods will apply to these larger structures also, and the thermochemical data in Table 1 should be interpreted accordingly. (Note that this disparity between computational methods appears to apply only to the BDE values for CO_2 within bicarbonate-containing structures: the BDE for removal of the H_2O ligand from $\text{H}_2\text{O}\cdot\text{Mg}^+\text{O}_2\text{COH}$ shows very good agreement between the CP-MP2(thaw)/B4G and CP-G2thaw values, and there is no reason to believe that any of the CP-MP2(thaw)B4G hydration energies are subject to significant error.)

3.2. Adduct ion structures and energetics for the species $\text{Mg}^+\cdot(\text{H}_2\text{O})_3\cdot\text{CO}_2$ and $\text{HOMg}^+\cdot(\text{H}_2\text{O})_3\cdot(\text{CO}_2)_i$ ($i = 0, 1$)

Total energies and BDE values for the various triply hydrated species are detailed in Table 1. Structures of the relevant OH-containing species are shown in Fig. 3. As might be expected, the increasing molecular complexity results in a proliferation of stationary points compared to the less hydrogenated systems. For example, two quite different structures are found for $\text{Mg}^+\cdot(\text{OH})_3\cdot\text{CO}_2$: one features all four ligands directly coordinated to Mg^+ , while the other has CO_2 coordinated instead to two of the water ligands. An entirely analogous dimorphism is evident also for $\text{HOMg}^+\cdot(\text{OH})_3\cdot\text{CO}_2$. For both $\text{Mg}^+\cdot(\text{OH})_3\cdot\text{CO}_2$ and $\text{HOMg}^+\cdot(\text{OH})_3\cdot\text{CO}_2$, the structure with all ligands within the first ‘solvent shell’ is the lower-energy isomer, but for $\text{Mg}^+\cdot(\text{OH})_3\cdot\text{CO}_2$ the difference in energy between the “4,0”

and “3,1” isomers is very small and could well be overturned through calculations at a higher level of theory. This result can be compared with calculations which have been performed on $\text{Mg}^+\cdot(\text{OH})_4$, which also reveal the existence of separate “4,0” and “3,1” isomers, but which suggest that the “3,1” structure is for that case the lower-energy species [40–42]. The competition between “4,0” and “3,1” structures in these systems reflects the interplay between metal ion/ligand attraction (which is clearly stronger at a smaller distance) and inter-ligand repulsion, due to steric effects as well as unfavorable dipole/dipole orientations (which are also a stronger, destabilising, influence at closer metal/ligand separations). In contrast, for $\text{HOMg}^+\cdot(\text{OH})_3\cdot\text{CO}_2$ the energetic ranking between “5,0” and “4,1” structures is much less ambiguous. The clear preference for the “5,0” isomer here is symptomatic of the much stronger interaction of HOMg^+ , than of bare Mg^+ , with ligands in the first solvent shell: removal of one ligand from this shell, in a complex of this size, carries too great an energetic cost to be adequately compensated for by the dilution of ligand/ligand repulsion effects.

For $\text{HOMg}^+\cdot(\text{OH})_3\cdot\text{CO}_2$ there are other structural subtleties also. Fig. 3 shows the “5,0” structure to be a moderately-distorted trigonal bipyramid, with CO_2 and one H_2O as the axial ligands. However, other minima exist which variously combine equatorial CO_2 and axial OH; both CO_2 and OH axial; and both CO_2 and OH equatorial. All of these “5,0” minima, for which interconversion by Berry pseudorotation (and, in some cases, intra-cluster proton transfer) is presumably facile, are separated by less than 5 kJ mol^{-1} in total: the structure shown in Fig. 3 (and included in Table 1) is the lowest in energy, by slightly more than

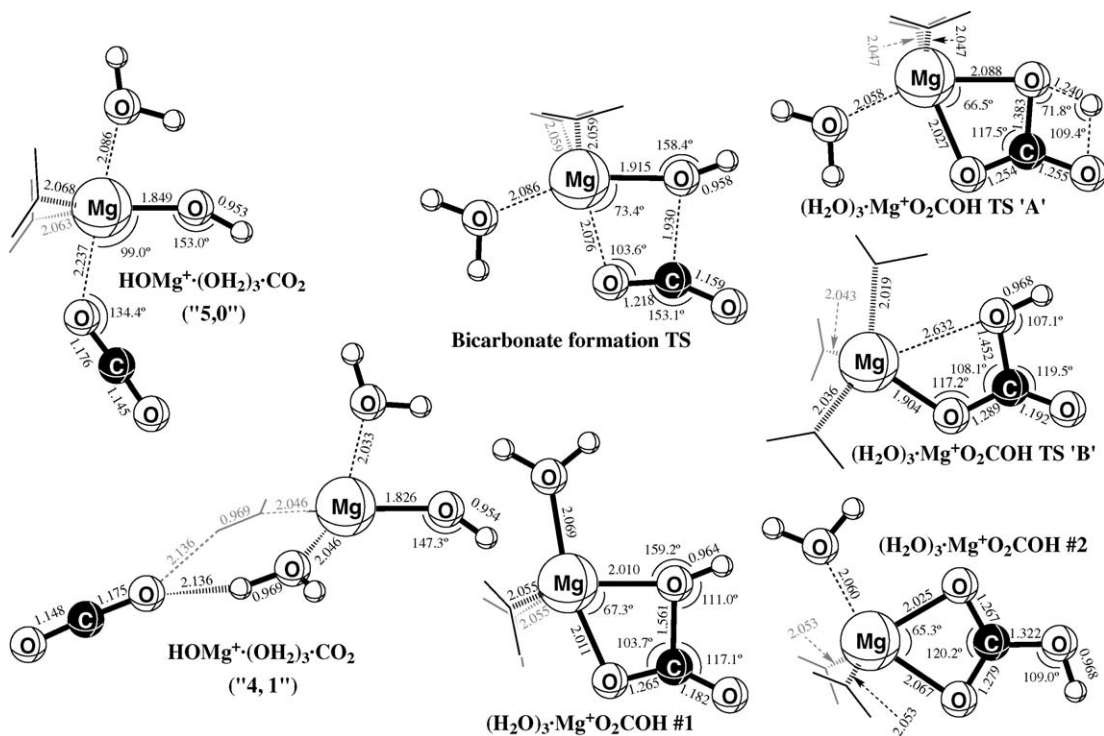


Fig. 3. Optimized geometries, obtained at the B3-LYP/6-311 + G** level of theory, of relevant minima and transition states of the structures $\text{HOMg}^+\cdot(\text{OH})_3\cdot\text{CO}_2$ and $(\text{H}_2\text{O})_3\cdot\text{Mg}^+\text{O}_2\text{COH}$. Bond lengths are shown in Ångstroms and bond angles in degrees. In most cases, out-of-plane water ligands are shown simply in stick form for simplicity; when such ligands lie behind the plane of the page, they are shown in half-tone.

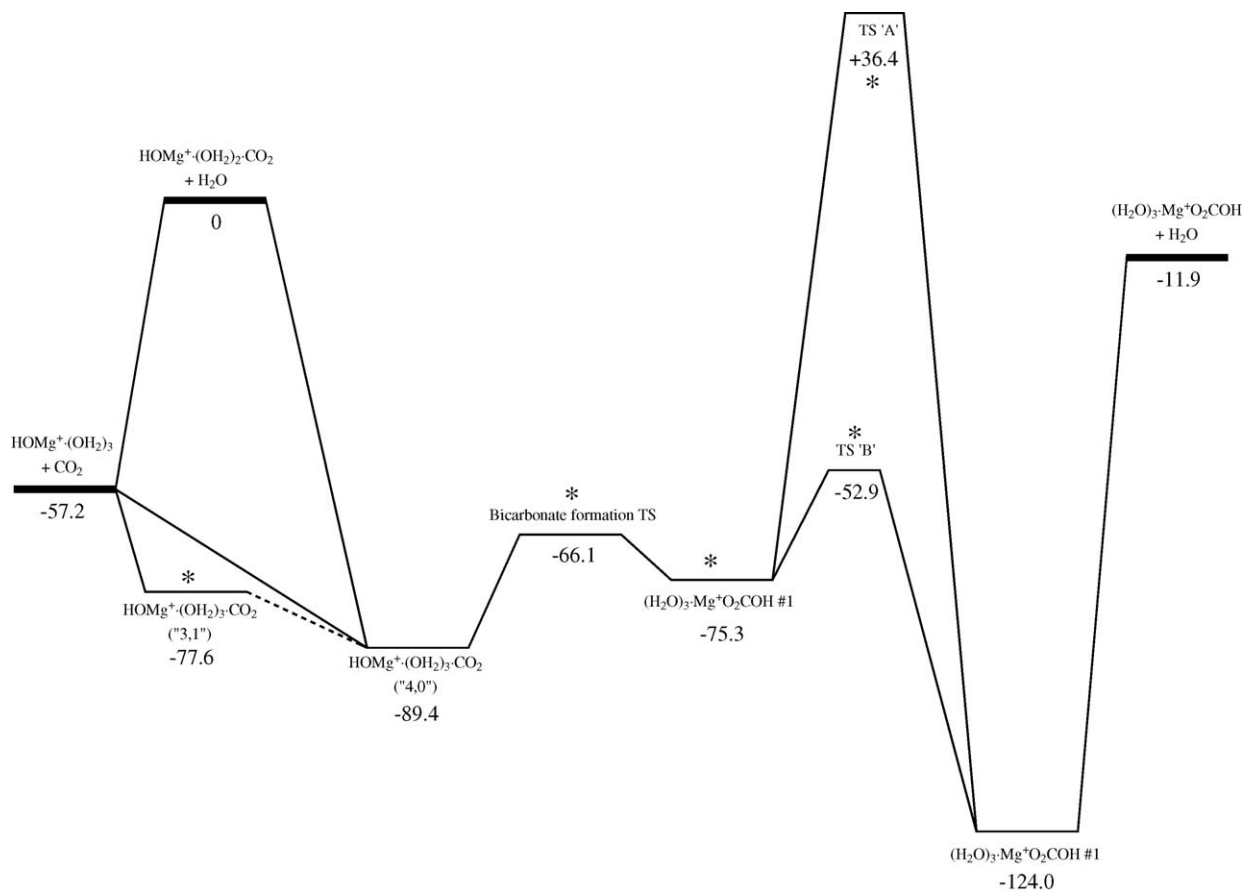


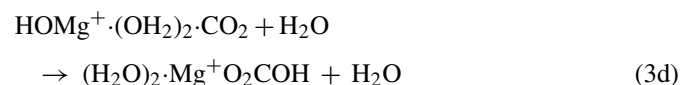
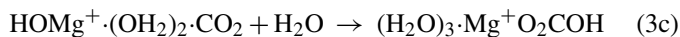
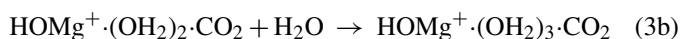
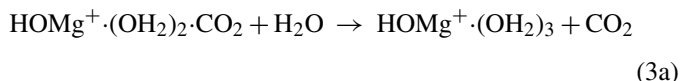
Fig. 4. Schematic diagram of relevant stationary points on the $\text{MgCH}_9\text{O}_7^+$ potential energy surface, showing opportunities for ligand switching, addition, and isomerization initiated by the reaction of $\text{HOMg}^+(\text{OH}_2)_2\cdot\text{CO}_2$ with H_2O . Bimolecular reactant and product combinations are identified by a bold line. Pathways shown with a dashed line are those for which a transition state has not been located but is expected to exist. Energies, expressed relative to reactant $\text{HOMg}^+(\text{OH}_2)_2\cdot\text{CO}_2 + \text{H}_2\text{O}$, are given in kJ mol^{-1} and are obtained from calculations at the CP-MP2(thaw)/B4G level of theory; note that the relative energies shown here have not been corrected for the 14.2 kJ mol^{-1} disparity between the CP-MP2(thaw)/B4G and CP-dG2thaw methods for bicarbonate CO_2 BDE values. Stationary points which have no identifiable counterparts at lower hydration numbers are denoted by an asterisk.

1 kJ mol^{-1} , at the CP-MP2(thaw)/B4G level of theory. The existence of other conformational isomers is evident also for several of the other structures shown in Fig. 3. In all cases, the energy difference between conformers is less than 5 kJ mol^{-1} , and we have detailed only the lowest-lying conformer of each structure type in Fig. 3 and in Table 1.

Perusal of the potential energy surface shown in Fig. 4 reveals that addition of a third H_2O ligand has achieved what the first two could not: activation of the pathway to bicarbonate ligand formation. How does this occur? It is apparent that the $(\text{H}_2\text{O})_3\cdot\text{Mg}^+\text{O}_2\text{COH}$ #2 isomer is the lowest-energy structure of those surveyed, and is apparently the global minimum: however, the doubly- and singly-hydrated bicarbonate-containing ions are also lower in energy than the corresponding $\text{HOMg}^+(\text{OH}_2)_n\cdot\text{CO}_2$ isomer. The energy difference between these isomers, for hydration number $n=1-3$, is respectively, 2.9, 26.2, and 49.3 kJ mol^{-1} , with the latter two values corrected by the increment of 14.2 kJ mol^{-1} corresponding to the observed discrepancy between CP-MP2(thaw)/B4G and CP-dG2thaw CO_2 BDEs for $n=0, 1$ as described in the preceding section. There is thus a clearly growing thermodynamic driving force to bicarbonate formation with increasing hydration num-

ber, but it is not solely this trend which results in bicarbonate formation for $n=3$. Rather, the activation of the bicarbonate formation pathway appears to be a consequence of two related effects: first, the gradual dilution in metal ion/ligand bond strengths, particularly the $\text{HOMg}^+(\text{OH}_2)_n\text{--CO}_2$ BDE term, with increasing n ; and second, the steady reduction in the $(\text{H})\text{OMgO}(\text{CO})$ angle from 180° to 99° as n is increased from 0 to 3. Both of these trends result from the increasing influence of the water ligands on the ligand/ligand repulsion term in the increasingly congested environment of the first solvent shell. The formation of an O–C bond between OH and CO_2 ligands, resulting in the initial production of the higher-energy bicarbonate isomer #1, is presumably encouraged by the comparatively close proximity of these two ligands within the lowest-energy conformer of $\text{HOMg}^+(\text{OH}_2)_3\cdot\text{CO}_2$, and yields a reduction in the ligand/ligand repulsion between H_2O ligands as the coordination environment around Mg is converted from distorted trigonal bipyramidal to something approximately tetrahedral. Once isomer #1 is formed, interconversion to the global minimum #2 can then occur by migration of $(\text{H}_2\text{O})_3\cdot\text{Mg}^+$ around the bicarbonate ligand in a manner entirely analogous to that already characterized for the reaction of $\text{NaOH} + \text{CO}_2$.

Although the calculations reported here show that bicarbonate formation is a feasible outcome of the reaction of $\text{HOMg}^+(\text{OH}_2)_2\text{CO}_2 + \text{H}_2\text{O}$, it is not possible to reliably determine the branching ratio of this reaction, in which ligand switching, association, and isomerization are all possible product channels:



The ligand switching process (3a), resulting in coordination of H_2O and loss of CO_2 , is the more exothermic bimolecular product channel, and is also more direct: it may therefore dominate over the H_2O -catalyzed formation of $(\text{H}_2\text{O})_2\text{Mg}^+\text{O}_2\text{COH}$ (3d), or the associative production of $\text{HOMg}^+(\text{OH}_2)_2\text{CO}_2$ or $(\text{H}_2\text{O})_3\text{Mg}^+\text{O}_2\text{COH}$. This may not, however, be the case for the reaction of more highly hydrated $\text{HOMg}^+(\text{OH}_2)_n\text{CO}_2$ clusters with H_2O , as the factors influencing bicarbonate formation (outlined above) are likely to grow in importance as the hydration number n is increased. If, as seems probable, the channel analogous to (3d) becomes progressively energetically more favorable (relative to the (3a) analogue) as the hydration number n increases, the situation will ultimately arise for some n where the most exothermic bimolecular product channel for the reaction of $\text{HOMg}^+(\text{OH}_2)_n\text{CO}_2$ with H_2O is the catalytic conversion, by H_2O , of the hydroxide and CO_2 ligands to bicarbonate.

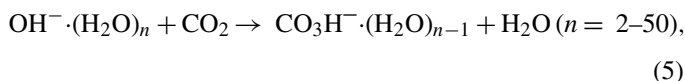
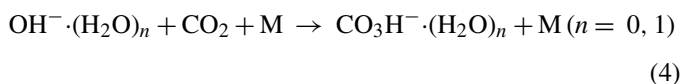
3.3. General discussion

It has long been appreciated that there are substantial and widespread differences between the chemical reactivity of species within the gas phase and in aqueous solution. These differences arise both from the ability of water, as a polar liquid with a high dielectric constant, to very substantially stabilize charged species (in particular, multiply charged species) and from the major difference in transport properties within solution versus the gas phase. However, it has only recently become possible to study the onset of the solvation process, by examining species within an environment in which only a few water molecules are present. Several instances have now been identified of bimolecular gas-phase reactions in which the product channel or reaction rate is very dramatically influenced by the number of solvent molecules associated with one of the reactants [43,44]. For example, hydration of gas-phase OH^- has a dramatic effect in reducing the rate of the $\text{S}_{\text{N}}2$ reaction with alkyl halides, although the reaction remains exothermic [45,46]. As another example from experimental studies, the benzene cation C_6H_6^+ , which is not stable in solution, will add six water molecules before its hydrophobic personality triumphs: on step-wise addition of the seventh or eighth H_2O , proton transfer to

the water cluster occurs leaving the acid-solvated phenyl radical $\text{C}_6\text{H}_5\cdot\text{H}_3\text{O}^+(\text{H}_2\text{O})_n$ [47]. Theoretical methods have also been widely used in recent years to examine slightly hydrated species, with the ‘onset’ of solvation (as diagnosed by a significant difference in the chemical behaviour of the solvated species versus the gas-phase condition) occurring, in several cases, surprisingly soon. For example, HOCN is stable against proton transfer to NH_3 in the gas phase, but relinquishes its proton to form the ion pair $\text{OCN}^-\text{NH}_4^+$ in the presence of only three water molecules [48]. A similar phenomenon occurs with NaOH , which is a robust closed-shell molecule within the gas phase but which converts to a solvated ion pair structure Na^+OH^- after, again, addition of only three H_2O ligands [19]. Other instances of charge separation have been described (for example in hydrated salts [49]), as also have water-assisted bond-forming reactions such as that between HCOOH and NH_3 [50]. A common feature in most of the theoretical studies to date is that the identified reactions involve H_2O as an active participant, through the formation of hydrogen bonds to one or both reactants, and it is often the influence of this hydrogen bonding network which is key to removing an activation energy barrier to the reaction. In contrast, in the present work, the reaction under investigation shows little tendency towards any influence of hydrogen bonding by the solvent molecules: rather, the present system is characterized by a ‘solvent effect’ which is more steric than anything else, in the sense that it is the crowding of solvent molecules around the central metal ion which appears to drive the reaction. As noted in the preceding section, the reaction of $\text{HOMg}^+(\text{OH}_2)_2\text{CO}_2 + \text{H}_2\text{O}$ can be considered as catalytic in the sense that one of the feasible product channels is $(\text{H}_2\text{O})_2\text{Mg}^+\text{O}_2\text{COH} + \text{H}_2\text{O}$. What is remarkable about this possible example of catalysis, as noted above, is the largely passive role of the H_2O reactant and product which contrasts sharply with, for example, the very active participation of the water molecule as a proton transfer agent in several instances of proton transport catalysis [51–54].

It would be of interest to characterize the influence of solvent molecules other than H_2O (for example, perhaps NH_3 or $(\text{CH}_3)_3\text{N}$) on formation of the $\text{Mg}^+\text{O}_2\text{COH}$ core: if, as we suggest, this is a largely steric effect, then a comparable degree of crowding by other solvent molecules should have a similar influence on the accessibility of bicarbonate ligand formation.

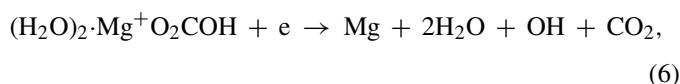
The present results can also be contrasted with a closely related system which has received repeated experimental study [55–57]: namely, the reactions



which are found to occur rapidly and without any apparent barrier across the full range of hydration numbers surveyed in the experiments. The lack of any discernible solvent effect in reactions (4) and (5) is understandable given that these reactions are presumably not subject to the constraints of the metal hydroxide reaction mechanism, in which it is necessary to first form a

less strongly coordinated metal bicarbonate ion (#1) which must then rearrange to the preferred isomer (#2).

Finally, it is worth commenting on the implications of the $\text{HOMg}^+(\text{H}_2\text{O})_n\cdot\text{CO}_2$ potential energy surface in the context of meteoric metal ion chemistry. As has been previously suggested [8,9], HOMg^+ is expected to be a key species resulting from the reactions of Mg^+ (produced through ablation of meteors within the upper atmosphere) with trace atmospheric constituents. Repeated association of HOMg^+ with atmospheric H_2O and CO_2 will ultimately produce cluster ions of sufficient size that the bicarbonate ligand formation channel is activated, and it is likely that the robust MgO_2COH fragment will survive neutralization of the larger cluster ions, producing a neutral radical which is itself likely to be efficient at adding water molecules. A simple calculation suggests that the ‘prototypical’ magnesium bicarbonate ion $(\text{H}_2\text{O})_2\cdot\text{Mg}^+\text{O}_2\text{COH}$ may well be just large enough to furnish intact MgO_2COH on recombination, as follows. The ionization energy of Mg, $\text{IE} = 7.646 \text{ eV}$, dictates that recombination of $\text{Mg}^+ + e$ releases 738 kJ mol^{-1} of energy. Loss of two water molecules, OH, and CO_2 from $(\text{H}_2\text{O})_2\cdot\text{Mg}^+\text{O}_2\text{COH}$, on recombination,



is mildly endothermic (by approximately 12 kJ mol^{-1} as determined from the Mg^+ recombination energy, the BDE values indicated in Table 1, and the value of $\text{BDE}(\text{Mg}^+-\text{OH}) = 314 \text{ kJ mol}^{-1}$ reported in Ref. [8]), suggesting that such extensive dissociation cannot occur on recombination. Thus, recombination of $(\text{H}_2\text{O})_2\cdot\text{Mg}^+\text{O}_2\text{COH}$ is expected to yield at least one larger fragment, which we would argue is more likely to be the relatively strongly-bound radical MgO_2COH (or perhaps MgOH) than any of the weakly-bound species $(\text{H}_2\text{O})_2$, $\text{H}_2\text{O}\cdot\text{CO}_2$, or $\text{HO}\cdot\text{CO}_2$. The steady augmentation of cumulative BDE values for $(\text{H}_2\text{O})_n\cdot\text{Mg}^+\text{O}_2\text{COH}$ ($n = 3, 4, 5, \dots$), increasing more steeply than the cumulative BDE values of clusters comprised solely of H_2O , CO_2 , and OH, makes it progressively more probable (as n increases) that $(\text{H}_2\text{O})_n\cdot\text{Mg}^+\text{O}_2\text{COH}$ recombines with retention of the MgO_2COH moiety. A crude (and arguably conservative) model of Mg^+ mesospheric chemistry, dealing with the formation of dihydrated HOMg^+ [8], suggests that the formation of ions such as $\text{HOMg}^+(\text{OH}_2)_2$ is reasonably efficient at altitudes of 80 km and below, and the proposed bicarbonate-containing ions can presumably arise at similar altitudes.

The prospects for survival of the MgO_2COH fragment, against parent ion recombination, implies a role for meteoric magnesium which is similar to that of sodium: the sodium bicarbonate molecule has been proposed to be one of the principal starting points for noctilucent cloud nucleation [1]. Magnesium is the main-group metal of highest abundance within meteoric material, and while it does not ablate so readily as, for example, the alkali metals Na and K, Mg^+ is nonetheless identified as one of the predominant upper-atmospheric metal ions. Therefore, the extent to which MgO_2COH and related species participate in the processing of water molecules within the upper atmosphere is a subject warranting serious study.

4. Conclusions

Bicarbonate formation, which occurs without effort in the gas-phase reactions of both bare OH^- and NaOH with CO_2 , does not occur in the reaction of HOMg^+ with CO_2 . However, successive hydration of the magnesium-containing ion is found to ‘unlock’ the formation of the bicarbonate ligand, through a process which is dominated by the increasing steric crowding of magnesium’s first solvent shell (and the relief of this crowding through bond formation between the hydroxide and CO_2 ligands). This influence of water molecules on reactivity differs from most of the other theoretical studies of solvation, which tend to highlight the importance of hydrogen-bonded network formation for bond activation or ion transport. Further study on solvation in other metal-containing systems is needed before the generality of this trend (in the steric activation of metal-centered reactions) can be properly assessed.

Acknowledgement

This work made extensive use of the supercomputing resources of the Australian Partnership of Advanced Computing, housed at the ANU Supercomputer Facility.

References

- [1] J.M.C. Plane, *Ann. Geophys.* 18 (2000) 807.
- [2] J.W. Ager, C.J. Howard, *J. Geophys. Res.* 92 (1987) 6675.
- [3] J.M.C. Plane, *Atmos. Chem. Phys.* 4 (2004) 627.
- [4] J.W. Ager, C.J. Howard, *J. Chem. Phys.* 87 (1987) 921.
- [5] J.M.C. Plane, C.-F. Nien, M.R. Allen, M. Helmer, *J. Phys. Chem.* 97 (1993) 4459.
- [6] R.M. Cox, J.M.C. Plane, *Phys. Chem. Chem. Phys.* 1 (1999) 4713.
- [7] P. Soldan, E.P.F. Lee, S.D. Gamblin, T.G. Wright, *Chem. Phys. Lett.* 313 (1999) 379.
- [8] S. Petrie, *Environ. Chem.* 2 (2005) 25.
- [9] B.R. Rowe, D.W. Fahey, E.E. Ferguson, F.C. Fehsenfeld, *J. Chem. Phys.* 75 (1981) 3325.
- [10] W.J. McNeil, S.T. Lai, E. Murad, *J. Geophys. Res.* 101 (1996) 5251.
- [11] C.G. Fesen, J.C. Gerard, P.B. Hays, D.N. Anderson, *J. Geophys. Res.* 102 (1997) 11673.
- [12] J. Fritzenwallner, E. Kopp, *Adv. Space Res.* 21 (1998) 859.
- [13] J. Kazil, E. Kopp, S. Chabrilat, J. Bishop, *J. Geophys. Res.* 108 (2003) 4432.
- [14] S. Petrie, *J. Phys. Chem. A* 106 (2002) 7034.
- [15] S. Petrie, *Int. J. Mass Spectrom.* 227 (2003) 33.
- [16] S. Petrie, *Aust. J. Chem.* 56 (2003) 259.
- [17] S. Petrie, *J. Phys. Chem. A* 107 (2003) 10441.
- [18] S. Petrie, *Icarus* 171 (2004) 199.
- [19] S. Petrie, *Environ. Chem.* 1 (2004) 35.
- [20] S. Petrie, *Environ. Chem.* 2 (2005) 308.
- [21] J. Bloomfield, E. Davies, P. Gatt, S. Petrie, *J. Phys. Chem. A* 110 (2006) 1134.
- [22] S. Petrie, *J. Phys. Chem. A* 105 (2001) 9931.
- [23] S. Petrie, *J. Phys. Chem. A* 106 (2002) 5188.
- [24] L.A. Curtiss, K. Raghavachari, G.W. Trucks, J.A. Pople, *J. Chem. Phys.* 94 (1991) 7221.
- [25] F.M. Siu, N.L. Ma, C.W. Tsang, *J. Chem. Phys.* 114 (2001) 7045.
- [26] S.F. Boys, F. Bernardi, *Mol. Phys.* 19 (1970) 553.
- [27] S. Petrie, *J. Phys. Chem. A* 102 (1998) 6138.
- [28] C. Lee, W. Yang, R.G. Parr, *Phys. Rev. B* 37 (1988) 785.
- [29] A.D. Becke, *J. Chem. Phys.* 98 (1993) 5648.
- [30] T.B. McMahon, G. Ohanessian, *Chem. Eur. J.* 6 (2000) 2931.

- [31] T.B. McMahon, *Int. J. Mass Spectrom.* 200 (2000) 187.
- [32] S. Hoyau, K. Norrman, T.B. McMahon, G. Ohanessian, *J. Am. Chem. Soc.* 121 (1999) 8864.
- [33] R.C. Dunbar, S. Petrie, *J. Phys. Chem. A* 109 (2005) 1411.
- [34] B.H. Wells, S. Wilson, *Chem. Phys. Lett.* 101 (1983) 429.
- [35] P. Valiron, I. Mayer, *Chem. Phys. Lett.* 275 (1997) 46.
- [36] K. Mierzwicki, Z. Latajka, *Chem. Phys. Lett.* 380 (2003) 654.
- [37] M.J. Frisch, G.W. Trucks, H.B. Schegel, G.E. Scuseria, M.A. Robb, J.R. Cheeseman, V.G. Zakrzewski, J.A. Montgomery Jr., R.E. Stratmann, J.C. Burant, S. Dapprich, J.M. Millam, A.D. Daniels, K.N. Kudin, M.C. Strain, O. Farkas, J. Tomasi, V. Barone, M. Cossi, R. Cammi, B. Mennucci, C. Pomelli, C. Adamo, S. Clifford, J.W. Ochterski, G.A. Petersson, P.Y. Ayala, Q. Cui, K. Morokuma, D.K. Malick, A.D. Rabuck, K. Raghavachari, J.B. Foresman, J. Cioslowski, J.V. Ortiz, B.B. Stefanov, G. Liu, A. Liashenko, P. Piskorz, I. Komaromi, R. Gomperts, R.L. Martin, D.J. Fox, T. Keith, M.A. Al-Laham, C.Y. Peng, A. Nanayakkara, C. Gonzalez, M. Challacombe, P.M.W. Gill, B.G. Johnson, W. Chen, M.W. Wong, J.L. Andres, M. Head-Gordon, E.S. Replogle, J.A. Pople, GAUSSIAN98 (Rev. A.7), Gaussian, Inc., Pittsburgh, P.A., 1998.
- [38] M.J. Frisch, G.W. Trucks, H.B. Schegel, G.E. Scuseria, M.A. Robb, J.R. Cheeseman, J.A. Montgomery Jr., T. Vreven, K.N. Kudin, J.C. Burant, J.M. Millam, S.S. Iyengar, J. Tomasi, V. Barone, B. Mennucci, M. Cossi, G. Scalmani, N. Rega, G.A. Petersson, H. Nakatsuji, M. Hada, M. Ehara, K. Toyota, R. Fukuda, J. Hasegawa, M. Ishida, T. Nakajima, Y. Honda, O. Kitao, H. Nakai, M. Klene, X. Li, J.E. Knox, H.P. Hratchian, J.B. Cross, C. Adamo, J. Jaramillo, R. Gomperts, R.E. Stratmann, O. Yazyev, A.J. Austin, R. Cammi, C. Pomelli, J.W. Ochterski, P.Y. Ayala, K. Morokuma, G.A. Voth, P. Salvador, J.J. Dannenberg, V.G. Zakrzewski, S. Dapprich, A.D. Daniels, M.C. Strain, O. Farkas, D.K. Malick, A.D. Rabuck, K. Raghavachari, J.B. Foresman, J.V. Ortiz, Q. Cui, A.G. Baboul, S. Clifford, J. Cioslowski, B.B. Stefanov, G. Liu, A. Liashenko, P. Piskorz, I. Komaromi, R.L. Martin, D.J. Fox, T. Keith, M.A. Al-Laham, C.Y. Peng, A. Nanayakkara, M. Challacombe, P.M.W. Gill, B. Johnson, W. Chen, M.W. Wong, C. Gonzalez, J.A. Pople, Gaussian03, Revision C.02, Gaussian, Inc., Wallingford, CT, 2004.
- [39] A. Gapeev, R.C. Dunbar, *J. Phys. Chem. A* 104 (2000) 4084.
- [40] N.F. Dalleska, B.L. Tjelta, P.B. Armentrout, *J. Phys. Chem.* 98 (1994) 4191.
- [41] T. Asada, S. Iwata, *Chem. Phys. Lett.* 260 (1996) 1.
- [42] A. Andersen, F. Muntean, D. Walter, C. Rue, P.B. Armentrout, *J. Phys. Chem. A* 104 (2000) 692.
- [43] J.E. Bartmess, *Adv. Gas Phase Ion Chem.* 2 (1996) 193.
- [44] K. Takashima, J.M. Riveros, *Mass Spectrom. Rev.* 17 (1998) 409.
- [45] D.K. Bohme, G.I. Mackay, *J. Am. Chem. Soc.* 103 (1981) 978.
- [46] P.M. Hierl, A.F. Ahrens, M. Henchman, A.A. Viggiano, J.F. Paulson, D.C. Clary, *J. Am. Chem. Soc.* 108 (1986) 3142.
- [47] Y.M. Ibrahim, M. Meot-Ner (Mautner), E.H. Alshraeh, M.S. El-Shall, S. Scheiner, *J. Am. Chem. Soc.* 127 (2005) 7053.
- [48] J.Y. Park, D.E. Woon, *Astrophys. J.* 601 (2004) L63.
- [49] C. Dedonder-Lardeux, G. Grégoire, C. Jouvet, S. Martrenchard, D. Solgadi, *Chem. Rev.* 100 (2000) 4023.
- [50] D.E. Woon, *Int. J. Quantum Chem.* 88 (2002) 226.
- [51] J.W. Gault, H. Audier, J. Fossey, L. Radom, *J. Am. Chem. Soc.* 118 (1996) 6299.
- [52] J.W. Gault, L. Radom, *J. Am. Chem. Soc.* 119 (1997) 9831.
- [53] M.A. Collins, L. Radom, *J. Chem. Phys.* 118 (2003) 6222.
- [54] S. Simon, M. Sodupe, J. Bertran, *Theor. Chem. Acc.* 111 (2004) 217.
- [55] F.C. Fehsenfeld, E.E. Ferguson, *J. Chem. Phys.* 61 (1974) 3181.
- [56] P.M. Hierl, J.F. Paulson, *J. Chem. Phys.* 80 (1984) 4890.
- [57] X. Yang, A.W. Castleman, *J. Am. Chem. Soc.* 113 (1991) 6766.